JCTC Journal of Chemical Theory and Computation

Information-Guided Noise Reduction in Forward−Backward Semiclassical Dynamics

Jonathan Chen and Nancy Makri*

Department of Chemistry, University of Illinois, 601 S. Goodwin Avenue, Urbana, Illinois 61801, United States

Received August 5, 2010

Abstract: Information-guided noise reduction (IGNoR) [*Chem. Phys. Lett.* **2004**, *400*, 446], a procedure for reducing the statistical error in Monte Carlo integration of oscillatory functions, is generalized to cases where both the prototype function and remaining integrand are complex-valued. The method is applied to the forward−backward semiclassical dynamics approximation of time correlation functions. Illustrative calculations of velocity autocorrelation functions in supercritical argon and liquid neon are presented.

I. Introduction

The so-called sign problem presents a major challenge in the Monte Carlo (MC) integration of oscillatory functions.[1] In statistical and condensed matter physics, integrands of alternating sign occur primarily in equilibrium calculations of identical fermions (as a result of particle exchange to account for antisymmetry) and in quantum dynamical calculations (because of the phase interference in the time evolution operator). Currently, the severity of the sign problem restricts the application of quantum Monte Carlo and path integral Monte Carlo methods to high temperatures, short times, and/or small numbers of particles or necessitates the use of extraneous approximations.

Few attempts to overcome the sign problem have been reported. Blocking algorithms[2] minimize cancellation by grouping integrand points and performing the sum within each block with deterministic methods. By choosing the blocks judiciously, the variance of the block averages can be smaller than that of the original function, thus reducing cancellation in the Monte Carlo step. A different, fully Monte Carlo based approach is information-guided noise reduction[3] (IGNoR). This exploits the knowledge of the exact integral for a similar, prototypical highly oscillatory function. The Monte Carlo random walk samples the prototype function and the desired integrand, estimating the ratios of the positive and negative parts of the two functions. With that information, IGNoR replaces the raw Monte Carlo estimate of the negative part of the desired integral by a corrected estimate obtained from knowledge of the exact integral of the prototype function. If the original and prototype functions are very similar, the IGNoR procedure will by construction generate excellent statistics.

In addition to these quite general algorithms, there are several strategies for reducing the severity of the sign problem by smoothing the integrand. The majority of these approaches are by nature approximate methods, but a few can be classified as numerically exact. In the present paper, we focus on the IGNoR methodology, which is a general and strictly numerical scheme for improving the Monte Carlo statistics within a specific formulation, i.e., without altering the integrand.

Clearly, the choice of the prototype function in IGNoR is critical to the success of the algorithm. Thus, the most critical step in the application of the algorithm is the identification of a function that is as similar as possible to the given integrand but whose integral is known exactly or at least can be obtained numerically to high accuracy. In many quantum mechanical methods, the prototype function must be chosen as a complex-valued part of the integrand. Thus, we generalize the original IGNoR methodology to the case of complex functions, pointing out that application of the noise reduction procedure to separate (ungrouped) terms is highly beneficial.

In section II, we review the IGNoR methodology and extend it to complex-valued integrands. Section III shows how the IGNoR correction may be applied to the calculation of time correlation functions within the forward−backward semiclassical dynamics (FBSD) approximation. The same

* Corresponding author e-mail: nancy@makri.scs.uiuc.edu.

10.1021/ct1004356
Published on Web 12/13/2010

section presents applications to the time correlation function of liquids, which demonstrates the dramatic decrease in statistical error attainable with the IGNoR procedure. Finally, some concluding remarks are given in section IV.

II. Information-Guided Noise Reduction for Complex Functions

a. IGNoR for Real Functions. The goal is to evaluate the (definite) integral J of an oscillatory function using a Monte Carlo procedure.[4] We start by expressing the desired integral in the form

$$J = \int f(x)\, g(x)\, \mathrm{d}x \tag{2.1}$$

where $f(x)$ is a reference function that is highly oscillatory, $g(x)$ is slowly varying, and the value of the integral

$$I = \int f(x)\, \mathrm{d}x \tag{2.2}$$

is known in advance. IGNoR exploits the helpful information in eq 2.2 to decrease the statistical error of the raw Monte Carlo estimate of eq 2.1.

First, I and J are split into their "signed" parts:

$$I_{\pm} = \int f(x)\, h(\pm f(x))\, \mathrm{d}x \tag{2.3}$$

$$J_{\pm} = \int f(x)\, g(x)\, h(\pm f(x))\, \mathrm{d}x \tag{2.4}$$

where

$$h(z) = \begin{cases} 0 & z < 0 \\ 1 & z \geq 0 \end{cases} \tag{2.5}$$

denotes the Heaviside step function. Next, the Monte Carlo random walk with a convenient sampling function is performed to obtain estimates $\langle I_{\pm}\rangle$ and $\langle J_{\pm}\rangle$ of the integrals 2.3 and 2.4. In the raw Monte Carlo procedure, the estimate of the desired integral is obtained by the simple addition

$$\langle J\rangle = \langle J_+\rangle + \langle J_-\rangle \tag{2.6}$$

The sign problem occurs because the positive and negative parts are comparable in absolute value, and their sum typically is smaller than the statistical error in their estimates. To improve the situation, IGNoR replaces $\langle J_-\rangle$ by the corrected value given by

$$\tilde{J}_- = \frac{\langle J_-\rangle}{\langle I_-\rangle}(I - \langle I_+\rangle) \tag{2.7}$$

Thus, the IGNoR-corrected estimate of the integral of interest is[3]

$$\langle J_+\rangle + \tilde{J}_- = \langle J_+\rangle + \frac{\langle J_-\rangle}{\langle I_-\rangle}(I - \langle I_+\rangle) \tag{2.8}$$

Because $\langle I_{\pm}\rangle$ and $\langle J_{\pm}\rangle$ are computed from the same random walk, these estimates are correlated; thus the error in the ratio $\langle J_-\rangle/\langle I_-\rangle$ generally is small. In fact, in the special case where $g(x) = a$ is a real constant, because the estimates $\langle I_{\pm}\rangle$ and $\langle J_{\pm}\rangle$ are obtained from the same random walk, $\langle J_-\rangle/\langle I_-\rangle = a$ exactly, and thus

$$\langle J_+\rangle + \tilde{J}_- = a\langle I_+\rangle + aI - a\langle I_+\rangle = aI = J \tag{2.9}$$

i.e., the IGNoR estimate 2.8 is exact. For nonconstant but slowly varying $g(x)$, eq 2.8 should be more accurate than the brute Monte Carlo estimate $\langle J_+\rangle + \langle J_-\rangle$.

We note that the procedure requires knowledge of the normalization integral of the MC sampling function. The latter must be available either exactly, or at least with much higher precision (smaller statistical uncertainty) than $\langle I_{\pm}\rangle$. Recovery of the exact integral value of 2.9 in the case of constant g holds only if the exact value of the MC normalization integral is known.

Finally, we note that eq 2.9 can be symmetrized,[5] leading to the prescription

$$\frac{1}{2}[\langle J_+\rangle + \tilde{J}_- + \langle J_-\rangle + \tilde{J}_+] \tag{2.10}$$

taking care to remember that partial error cancellation is achieved through the *pairings* $\langle J_+\rangle + \tilde{J}_-$ and $\langle J_-\rangle + \tilde{J}_+$, as evident through eq 2.9. The symmetrized IGNoR prescription may offer some advantages, although unsymmetrized and symmetrized formulas produced very similar results in the calculations reported in section III.

b. IGNoR for Complex Functions. To extend IGNoR to cases where both functions are complex-valued, one needs to separate the integrand into appropriate real and imaginary parts. One may split the product fg into its real and imaginary components, resulting in two integrals to be calculated by IGNoR. A second choice is to apply the IGNoR correction to each of the four terms in the product fg. An earlier application of IGNoR[6] used the first partitioning, which is not optimal, because the relevant functions are not necessarily strongly correlated. For example, in the special case where g is a complex-valued constant, the IGNoR based on splitting the product fg into real and imaginary parts does not lead to the exact result. Below, we describe the second partitioning, which is *designed* to have zero statistical error when g is a complex-valued constant and thus should be more accurate when $g(x)$ is a smooth complex-valued function.

We begin by separating the desired integral into four components arising from the real and imaginary parts of each of the two functions:

$$J = J^{\mathrm{rr}} - J^{\mathrm{ii}} + iJ^{\mathrm{ri}} + iJ^{\mathrm{ir}} \tag{2.11}$$

where

$$J^{\mathrm{rr}} = \int \mathrm{Re}\, f(x)\, \mathrm{Re}\, g(x)\, \mathrm{d}x,\ J^{\mathrm{ri}} = \int \mathrm{Re}\, f(x)\, \mathrm{Im}\, g(x)\, \mathrm{d}x,$$
$$J^{\mathrm{ir}} = \int \mathrm{Im}\, f(x)\, \mathrm{Re}\, g(x)\, \mathrm{d}x,\ J^{\mathrm{ii}} = \int \mathrm{Im}\, f(x)\, \mathrm{Im}\, g(x)\, \mathrm{d}x \tag{2.12}$$

We also write $I = I^{\mathrm{r}} + iI^{\mathrm{i}}$ and define the integrals of the positive and negative components of each integral:

$$I^{\mathrm{r}}_{\pm} = \int \mathrm{Re}\, f(x)\, h(\pm \mathrm{Re}\, f(x))\, \mathrm{d}x,$$
$$I^{\mathrm{i}}_{\pm} = \int \mathrm{Im}\, f(x)\, h(\pm \mathrm{Im}\ f(x))\, \mathrm{d}x \tag{2.13}$$

$$\begin{aligned} J_{\pm}^{\mathrm{rr}} &= \int \mathrm{Re}\, f(x)\, \mathrm{Re}\, g(x)\, h(\pm \mathrm{Re}\, f(x))\, \mathrm{d}x, \\ J_{\pm}^{\mathrm{ri}} &= \int \mathrm{Re}\, f(x)\, \mathrm{Im}\, g(x)\, h(\pm \mathrm{Re}\, f(x))\, \mathrm{d}x, \\ J_{\pm}^{\mathrm{ir}} &= \int \mathrm{Im}\, f(x)\, \mathrm{Re}\, g(x)\, h(\pm \mathrm{Im}\, f(x))\, \mathrm{d}x, \\ J_{\pm}^{\mathrm{ii}} &= \int \mathrm{Im}\, f(x)\, \mathrm{Im}\, g(x)\, h(\pm \mathrm{Im}\, f(x))\, \mathrm{d}x \end{aligned} \tag{2.14}$$

Now, we apply the original IGNoR procedure to each component of J:

$$\begin{aligned} \tilde{J}_{-}^{\mathrm{rr}} &= \frac{\langle J_{-}^{\mathrm{rr}} \rangle}{\langle I_{-}^{\mathrm{r}} \rangle}(I^{\mathrm{r}} - \langle I_{+}^{\mathrm{r}} \rangle), \tilde{J}_{-}^{\mathrm{ri}} = \frac{\langle J_{-}^{\mathrm{ri}} \rangle}{\langle I_{-}^{\mathrm{r}} \rangle}(I^{\mathrm{r}} - \langle I_{+}^{\mathrm{r}} \rangle), \\ \tilde{J}_{-}^{\mathrm{ir}} &= \frac{\langle J_{-}^{\mathrm{ir}} \rangle}{\langle I_{-}^{\mathrm{i}} \rangle}(I^{\mathrm{i}} - \langle I_{+}^{\mathrm{i}} \rangle), \tilde{J}_{-}^{\mathrm{ii}} = \frac{\langle J_{-}^{\mathrm{ii}} \rangle}{\langle I_{-}^{\mathrm{i}} \rangle}(I^{\mathrm{i}} - \langle I_{+}^{\mathrm{i}} \rangle) \end{aligned} \tag{2.15}$$

Since the IGNoR prescription is now performed on four real-valued integrands, eq 2.15 should yield the exact value of the desired integral in the case where g is a complex-valued constant. The numerical calculations reported in section III follow this procedure.

III. Application: Forward−Backward Semiclassical Dynamics of Liquids

Various simulation methods developed in the past decade are based on semiclassical ideas.[7] Semiclassical methods[8] are attractive because they employ classical trajectories to capture dynamical effects. Still, the highly oscillatory semiclassical phase leads to a severe sign problem, and fully semiclassical calculations in many-particle systems remain impractical. Certain semiclassical approximations to Heisenberg operators, which contain forward and reverse time evolution steps, take advantage of the proximity (in the stationary phase limit) of forward and backward trajectories to eliminate the oscillatory semiclassical phase altogether.[9] In the particular case of time correlation functions, such ideas give rise to linearized semiclassical[10,11] (LSC) and forward−backward[12,13] semiclassical dynamics (FBSD) approximations. However, even with this extremely important stabilization, the resulting expressions converge much slower than fully classical calculations. This is so because of the presence of oscillatory components through coherent state factors (in the case of FBSD) or the Wigner transformation (in the case of LSC approximations). Further, more accurate (and costly) semiclassical treatments have been formulated, which reintroduce a portion of the oscillatory semiclassical phase, thereby capturing some coherence features at the expense of numerical stability.[14] All of these situations invite the application of IGNoR to improve convergence. In this section, we illustrate the enhancement obtained by implementing the IGNoR methodology on FBSD calculations of velocity correlation functions in neat liquids.

Our present focus is on time correlation functions at a finite temperature, specifically the correlation function for the inner product of two vector operators $\hat{\mathbf{A}}$ and $\hat{\mathbf{B}}$

$$C_{\mathbf{A}\cdot\mathbf{B}}(t) = \frac{1}{Z} Tr(\mathrm{e}^{-\beta\hat{H}} \hat{\mathbf{A}}\, \mathrm{e}^{i\hat{H}t/\hbar} \cdot \hat{\mathbf{B}}\, \mathrm{e}^{-i\hat{H}t/\hbar}) \tag{3.1}$$

Here, $\hat{H}$ is the Hamiltonian that describes the n-particle system, $\hat{\mathbf{A}}$ and $\hat{\mathbf{B}}$ are vector operators, $\beta = 1/k_{\mathrm{B}}T$ is the reciprocal temperature, and $Z = Tr\, \mathrm{e}^{-\beta\hat{H}}$ is the canonical partition function. The three-dimensional Cartesian position and momentum vectors for the jth atom are denoted, respectively, as $\mathbf{r}_j = (r_{j1}, r_{j2}, r_{j3})$ and $\mathbf{p}_j = (p_{j1}, p_{j2}, p_{j3})$. For notational convenience, the coordinates and momenta of all of the particles are collected in the $3n$-dimensional vectors $\mathbf{Q}$ and $\mathbf{P}$, respectively. The Hamiltonian is written as

$$\hat{H} = \hat{T} + V(\hat{\mathbf{Q}}) \tag{3.2}$$

where $\hat{T}$ is the operator for the total kinetic energy of the system.

$$\hat{T} = \sum_{j=1}^{n} \hat{T}_j = \sum_{j=1}^{n} \frac{|\hat{\mathbf{p}}_j|^2}{2m_j} \tag{3.3}$$

Exponentiation of the operator $\hat{B}$ via a derivative identity and application of the forward−backward semiclassical idea in a coherent state representation[15] gives rise to the following FBSD approximation of eq 3.1:[13]

$$\begin{aligned} C_{\mathbf{A}\cdot\mathbf{B}}(t) \;=\; & (2\pi\hbar)^{-3n} Z^{-1} \int \mathrm{d}\mathbf{Q}^{(0)} \int \mathrm{d}\mathbf{P}^{(0)} \left(1 + \frac{3}{2}n\right) \langle G(\mathbf{Q}^{(0)}, \mathbf{P}^{(0)}) | \\ & | \mathrm{e}^{-\beta\hat{H}} \hat{\mathbf{A}} | G(\mathbf{Q}^{(0)}, \mathbf{P}^{(0)}) \rangle \cdot \mathbf{B}(\mathbf{Q}(t), \mathbf{P}(t)) \\ & - 2(2\pi\hbar)^{-3n} Z^{-1} \int \mathrm{d}\mathbf{Q}^{(0)} \int \mathrm{d}\mathbf{Q}^{(0)} \langle G(\mathbf{Q}^{(0)}, \mathbf{P}^{(0)}) | (\hat{\mathbf{Q}} - \mathbf{Q}^{(0)})\, \mathrm{e}^{-\beta\hat{H}} \\ & [\hat{\mathbf{A}} \cdot \mathbf{B}(\mathbf{Q}(t), \mathbf{P}(t))] \cdot \Gamma \cdot (\hat{\mathbf{Q}} - \mathbf{Q}^{(0)}) | G(\mathbf{Q}^{(0)}, \mathbf{P}^{(0)}) \rangle \end{aligned} \tag{3.4}$$

Here, $\mathbf{Q}^{(0)}$ and $\mathbf{P}^{(0)}$ are the initial phase space variables for classical trajectories that evolve according to the classical equations of motion corresponding to the product of three exponential operators, $\mathbf{Q}(t)$ and $\mathbf{P}(t)$ are the phase space variables at time t, and $\mathbf{B}(\mathbf{Q},\mathbf{P})$ is the classical analogue of the operator $\hat{\mathbf{B}}$. The ket in eq 3.4 represents a $3n$-dimensional coherent state,[16] i.e., a product of n three-dimensional coherent states for each particle, and is described in the coordinate representation by the wave function

$$\begin{aligned} \langle \mathbf{Q} | G(\mathbf{Q}^{(0)}, \mathbf{P}^{(0)}) \rangle \;&=\; \prod_{j=1}^{n} \langle \mathbf{r}_j | g(\mathbf{r}_j^{(0)}, \mathbf{p}_j^{(0)}) \rangle \\ &= \left(\frac{2}{\pi}\right)^{3n/4} (\det \boldsymbol{\Gamma})^{1/4} \times \\ &\quad \exp[-(\mathbf{Q} - \mathbf{Q}^{(0)})\, \boldsymbol{\Gamma}\, (\mathbf{Q} - \mathbf{Q}^{(0)}) + \\ &\quad \frac{i}{\hbar} \mathbf{P}^{(0)} (\mathbf{Q} - \mathbf{Q}^{(0)}) \end{aligned} \tag{3.5}$$

where $\boldsymbol{\Gamma}$ is a $3n \times 3n$ matrix. Throughout the rest of the paper, we choose a diagonal form with elements γ_j representing the width parameters of the coherent state for the jth particle. Typically, these values are chosen to match the characteristic frequencies of the system.

The next step to consider is the evaluation of the coherent state transform of the operators, both of which involve the Boltzmann operator. A fully quantum treatment of this time-independent part is essential in capturing the effects of zero-point energy and reproducing the imaginary part of a correlation function. An accurate evaluation of these matrix elements is possible[17−19] by using the discretized path

integral representation of the Boltzmann operator.[20] After some algebra, eq 3.4 becomes

$$C_{\mathbf{A}\cdot\mathbf{B}}(t) = (2\pi\hbar)^{-3n}Z^{-1} \times \int d\mathbf{Q}^{(0)} \int d\mathbf{P}^{(0)} \int d\mathbf{Q}^{(1)} ... \int d\mathbf{Q}^{(N)} \Theta(\mathbf{Q}^{(0)}, \mathbf{P}^{(0)}, \mathbf{Q}^{(1)}, ..., \mathbf{Q}^{(N)}) \Lambda_{\mathbf{A}\cdot\mathbf{B}}(\mathbf{Q}^{(0)}, \mathbf{P}^{(0)}, \mathbf{Q}^{(1)}, ..., \mathbf{Q}^{(N)};t) \quad (3.6)$$

In these equations, $\Delta\beta = \beta/N$,

$$\Theta(\mathbf{Q}^{(0)}, \mathbf{P}^{(0)}, \mathbf{Q}^{(1)}, ..., \mathbf{Q}^{(N)}) = \prod_{j=1}^{n}\left(\frac{2\gamma_j}{\pi}\right)^{3/2}\left(\frac{m_j}{m_j + \hbar^2\Delta\beta\gamma_j}\right)^3 \left(\frac{m_j}{2\pi\hbar^2\Delta\beta}\right)^{3(N-1)/2} \times \exp\left\{-\sum_{j=1}^{n}\frac{m_j}{m_j + \hbar^2\Delta\beta\gamma_j}\left(\gamma_j|\mathbf{r}_j^{(1)} - \mathbf{r}_j^{(0)}|^2 + \gamma_j|\mathbf{r}_j^{(N)} - \mathbf{r}_j^{(0)}|^2 + \frac{i}{\hbar}\mathbf{p}_j^{(0)}(\mathbf{r}_j^{(1)} - \mathbf{r}_j^{(N)}) + \frac{\Delta\beta}{2m_j}|\mathbf{p}_j^{(0)}|^2\right) - \sum_{j=1}^{n}\frac{m_j}{2\hbar^2\Delta\beta}\sum_{k=2}^{N}|\mathbf{r}_j^{(k)} - \mathbf{r}_j^{(k-1)}|^2 - \Delta\beta\sum_{k=1}^{N}V(\mathbf{Q}^{(k)})\right\} \quad (3.7)$$

is the integrand in the Trotter-discretized path integral representation of the coherent state transform of the Boltzmann operator, and the function $\Lambda_{\mathbf{A}\cdot\mathbf{B}}$ depends upon the form of the chosen operators. Recent work has focused on momentum autocorrelation functions, obtained with the choice $\hat{\mathbf{A}} = \hat{B} = \hat{\mathbf{p}}$. In that case, $\Lambda_{\mathbf{p}\cdot\mathbf{p}}$ is given by the expression[18]

$$\Lambda_{\mathbf{p}\cdot\mathbf{p}}(\mathbf{Q}^{(0)}, \mathbf{P}^{(0)}, \mathbf{Q}^{(1)}, ..., \mathbf{Q}^{(N)};t) = \left(1 + \frac{3}{2}n\right)\theta - 2\sum_{j=1}^{n}\sum_{\alpha=1}^{3}\gamma_j\varphi_{j\alpha}^{*}(r_{j\alpha}^{(0)}, p_{j\alpha}^{(0)}, r_{j\alpha}^{(1)})\left(-i\hbar\frac{m_j}{m_j + \hbar^2\Delta\beta\gamma_j}p_{j\alpha}(t) + \theta\varphi_{j\alpha}(r_{j\alpha}^{(0)}, p_{j\alpha}^{(0)}, r_{j\alpha}^{(N)})\right) \quad (3.8)$$

where

$$\varphi_{j\alpha}(r_{j\alpha}^{(0)}, p_{j\alpha}^{(0)}, r_{j\alpha}^{(k)}) = \frac{m_j}{m_j + \hbar^2\Delta\beta\gamma_j}\left(r_{j\alpha}^{(k)} - r_{j\alpha}^{(0)} + i\hbar\frac{\Delta\beta}{2m_j}p_{j\alpha}^{(0)}\right) \quad (3.9)$$

and

$$\theta = \sum_{j=1}^{n}\sum_{\alpha=1}^{3}\frac{m_j}{m_j + \hbar^2\Delta\beta\gamma_j}[p_{j\alpha}^{(0)} + 2i\hbar\gamma_j(r_{j\alpha}^{(N)} - r_{j\alpha}^{(0)})]\, p_{j\alpha}(t) \quad (3.10)$$

Equation 3.6 is a quasiclassical expression. From eqs 3.8 and 3.10, one can see that all time dependence in the FBSD correlation function arises from the classical momentum values $p_{j\alpha}(t)$.

The multidimensional integral appearing in eq 3.6 is performed by Monte Carlo (or, alternatively, a molecular dynamics procedure[21]). The Monte Carlo procedure commonly uses the modulus of the absolute value of the exponential part as the sampling function

$$\rho(\mathbf{Q}^{(0)}, \mathbf{P}^{(0)}, \mathbf{Q}^{(1)}, ..., \mathbf{Q}^{(N)}) = |\Theta(\mathbf{Q}^{(0)}, \mathbf{P}^{(0)}, \mathbf{Q}^{(1)}, ..., \mathbf{Q}^{(N)})| \quad (3.11)$$

In the single-bead ($N = 1$) case, the integral of this sampling function is proportional to the partition function, thus the normalization integral cancels out. However, this is not the case when $N > 1$, and one must perform a separate Monte Carlo calculation to normalize the results. This can be done efficiently using a straightforward procedure.[18]

Even in the single-bead limit, the integrand of the FBSD expression contains negative components. In addition, a mildly oscillatory factor

$$\prod_{j=1}^{n}\exp\left[-\frac{i}{\hbar}\frac{m_j}{m_j + \hbar^2\Delta\beta\gamma_j}\mathbf{p}_j^{(0)}(\mathbf{r}_j^{(1)} - \mathbf{r}_j^{(N)})\right] \quad (3.12)$$

is present when $N > 1$, which arises from the coherent state phase. Because these factors introduce phase cancellation, whose magnitude increases exponentially with the number of particles, the use of IGNoR should be beneficial.

We have found the IGNoR procedure for complex functions ideally suited to the present situation with the choice

$$f(\mathbf{Q}^{(0)}, \mathbf{P}^{(0)}, \mathbf{Q}^{(1)}, ..., \mathbf{Q}^{(N)}) = (2\pi\hbar)^{-3n}Z^{-1}\Theta(\mathbf{Q}^{(0)}, \mathbf{P}^{(0)}, \mathbf{Q}^{(1)}, ..., \mathbf{Q}^{(N)}) \Lambda_{\mathbf{p}\cdot\mathbf{p}}(\mathbf{Q}^{(0)}, \mathbf{P}^{(0)}, \mathbf{Q}^{(1)}, ..., \mathbf{Q}^{(N)};0) \quad (3.13)$$

$$g(\mathbf{Q}^{(0)}, \mathbf{P}^{(0)}, \mathbf{Q}^{(1)}, ..., \mathbf{Q}^{(N)}) = \frac{\Lambda_{\mathbf{p}\cdot\mathbf{p}}(\mathbf{Q}^{(0)}, \mathbf{P}^{(0)}, \mathbf{Q}^{(1)}, ..., \mathbf{Q}^{(N)};t)}{\Lambda_{\mathbf{p}\cdot\mathbf{p}}(\mathbf{Q}^{(0)}, \mathbf{P}^{(0)}, \mathbf{Q}^{(1)}, ..., \mathbf{Q}^{(N)};0)} \quad (3.14)$$

Because eq 3.13 is the integrand of the $t = 0$ expression, its integral is proportional to the equilibrium value of the kinetic energy

$$I = Z^{-1}Tr(e^{-\beta\hat{H}}\,\hat{\mathbf{p}}\cdot\hat{\mathbf{p}}) \quad (3.15)$$

and can be obtained by a high-precision path integral Monte Carlo calculation (which does not suffer from the dynamical sign problem). Further, the imaginary part of the integral is identically equal to zero. Here, we report the results of calculations on supercritical argon and liquid neon.

Figure 1 shows single-bead ($N = 1$) FBSD results for supercritical argon. The calculations were performed at 183 K and a density of 1.15 g cm^{-3} upon a cubic unit cell containing 108 atoms under periodic boundary conditions. All interactions were truncated at half of the unit cell dimensions and are described by a Lennard-Jones potential with $\varepsilon = 85$ cm^{-1} and $\sigma = 3.4$ Å, where r represents the interatomic separation.[22] Raw and IGNoR-corrected Monte Carlo results from calculations with only 10 000 trajectories are compared against earlier results using molecular dynamics sampling with 1 million trajectories. At $t = 0$, the partitioning described in eqs 3.13 and 3.14 results in $g = 1$, which guarantees, by construction, zero IGNoR error. However, Figure 1 shows that the statistical error of the IGNoR calculations remains small as the time increases. Although the integrand is not rapidly oscillatory in the single bead limit, where the problematic phase factor 3.12 reduces to unity, application of the IGNoR procedure described in the previous section results in considerable shrinking of statistical error, yielding meaningful results with a 100-fold

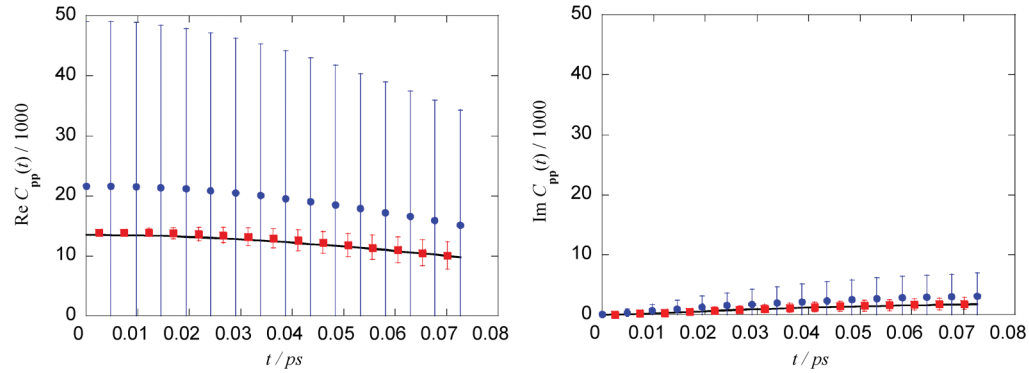

Figure 1. Velocity autocorrelation function of supercritical argon from FBSD calculations in the single-bead discretization of the Boltzmann operator. Blue and red markers show raw and IGNoR-corrected Monte Carlo results (along with error bars), respectively, from calculations with 10 000 trajectories. The black line shows equivalent results using molecular dynamics sampling with 1 million trajectories.

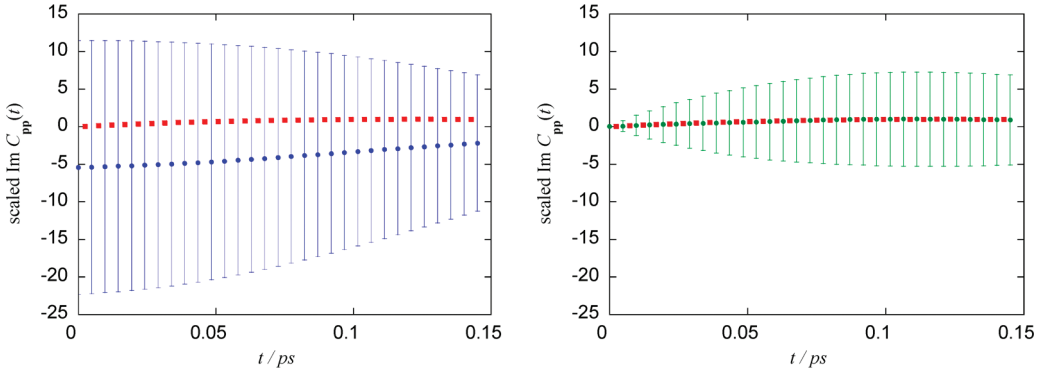

Figure 2. Velocity autocorrelation function of liquid neon from FBSD calculations with $N = 2$ using 8 million trajectories. (a) Raw (blue) and IGNoR-corrected (red) Monte Carlo results. (b) Comparison of IGNoR corrected results from the application of error correction to each term of the real and imaginary parts, as prescribed by eq 2.15 (red), vs application to the entire real and imaginary part of the correlation function (green). It is seen that the current procedure, where the IGNoR processing is applied to each term separately, leads to much better statistics. The error bars of the results obtained from the IGNoR procedure given by eq 2.15 are smaller than the size of the markers.

reduction in the number of trajectories compared to the earlier raw calculation.

Similar calculations were performed on liquid neon with parameters chosen to match the calculations of Lawrence et al. ($T = 29.9$ K and a density of 0.03755 Å^{-3}). Interactions between neon atoms were described by a Lennard-Jones potential with $\varepsilon = 35.6$ K and $\sigma = 2.749$ Å. In order to avoid performing additional Monte Carlo calculations required for normalization, the IGNoR-corrected results were scaled arbitrarily to have the maximum of each curve equal to unity. This is possible because $I^{i} = 0$ for FBSD autocorrelation functions.

Figure 2 shows (scaled) raw Monte Carlo and IGNoR-corrected FBSD results with $N = 2$ obtained from a calculation with 8 million trajectories. As seen in Figure 2a, the error reduction accomplished by applying the IGNoR procedure is much more dramatic compared to the single-bead calculation in Figure 1. This is so because negative integrand areas arise not only from $\Lambda_{\mathbf{p}\cdot\mathbf{p}}$ but also from factor 3.12, which makes phase cancellation much more prevalent. Also, Figure 2b shows that the current application of IGNoR, eq 2.15, where the noise reduction is applied to *each* term in the real and imaginary components, results in much better statistics.

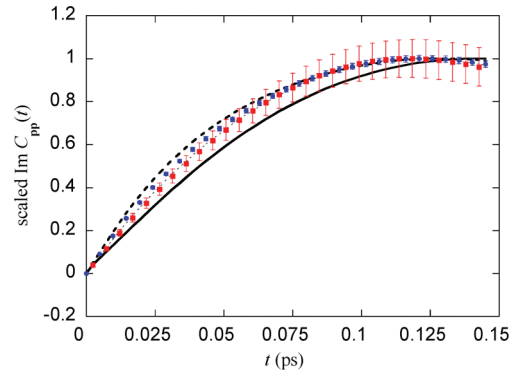

Figure 3. Velocity autocorrelation function of liquid neon from IGNoR-corrected FBSD calculations with $N = 1-4$ (black dashed line, blue circles, black dashed line and red squares, respectively) using 8 million trajectories. For clarity, error bars are shown only for $N = 2$ and 4. The black line shows FBSD results with the PPP single-bead discretization of the Boltzmann operator. All curves have been scaled to the same maximum.

Finally, Figure 3 shows similar (scaled) IGNoR-corrected FBSD results for $N = 1-4$. As the number of path integral beads is increased, the Trotter-discretized FBSD results approach those obtained in the single-bead PPP approxima-

tion to the Boltzmann operator.[22] An increase in the number of beads beyond $N = 1$, which was previously prohibitive computationally with these particular parameters because of dramatic phase cancellation, becomes feasible with modest numbers of trajectories by incorporating the IGNoR correction in the FBSD methodology.

IV. Concluding Remarks

We have presented an efficient extension of the IGNoR Monte Carlo methodology to complex-valued functions. The basic requirement of IGNoR is the identification of a function f that incorporates as much of the integrand (including the oscillatory components) as possible and whose integral is known accurately. If the remaining factor g of the integrand is sufficiently smooth, the IGNoR correction leads to a large reduction of statistical error compared to the raw Monte Carlo estimate. In the case of complex-valued functions, we find the application of IGNoR to each of the four terms arising from the real and imaginary parts of the product fg most effective.

The application of IGNoR to FBSD correlation functions in neat liquids led to a dramatic reduction of statistical error. When the Boltzmann operator is discretized using multiple path integral beads ($N > 1$), the FBSD integrand is oscillatory and its variance grows rapidly as the number of particles is increased. For certain parameters, the raw Monte Carlo evaluation of the FBSD expression becomes prohibitively expensive. The application of IGNoR reduced the statistical error by several orders of magnitude, making convergence feasible with modest amounts of computational effort.

Because our goal in this paper was assessing the improvement attainable through IGNoR, our calculations employed the primitive Trotter discretization. In addition, we refrained from performing the separate Monte Carlo calculation required to evaluate the normalization integral of the sampling function, reporting un-normalized results. Future work should incorporate the correct normalization constant and employ the more efficient pair-product propagator,[23,24] which will lead to much faster convergence of FBSD correlation functions in neat fluids.

References

(1) *Quantum Monte Carlo methods in condensed matter physics*; Suzuki, M., Ed.; World Scientific: Singapore, 1993.

(2) Mak, C. H.; Egger, R.; Gottschick, J. *Phys. Rev. Lett.* **1998**, *81*, 4533.

(3) Makri, N. *Chem. Phys. Lett.* **2004**, *400*, 446.

(4) Metropolis, N.; Rosenbluth, A. W.; Rosenbluth, M. N.; Teller, H.; Teller, E. *J. Chem. Phys.* **1953**, *21*, 1087.

(5) Jadhao, V. Private communication.

(6) Bukhman, E.; Makri, N. *J. Phys. Chem.* **2009**, *113*, 7183.

(7) Van Vleck, J. H. *Proc. Natl. Acad. Sci. U.S.A.* **1928**, *14*, 178.

(8) Miller, W. H. *Adv. Chem. Phys.* **1974**, *25*, 69.

(9) Makri, N.; Thompson, K. *Chem. Phys. Lett.* **1998**, *291*, 101.

(10) Wang, H.; Sun, X.; Miller, W. H. *J. Chem. Phys.* **1998**, *108*, 9726.

(11) Poulsen, J. A.; Nyman, G.; Rossky, P. J. *J. Chem. Phys.* **2003**, *119*, 12179.

(12) Sun, X.; Miller, W. H. *J. Chem. Phys.* **1999**, *110*, 6635.

(13) Shao, J.; Makri, N. *J. Phys. Chem. A* **1999**, *103*, 7753.

(14) Thoss, M.; Wang, H.; Miller, W. H. *J. Chem. Phys.* **2001**, *114*, 9220.

(15) Herman, M. F.; Kluk, E. *Chem. Phys.* **1984**, *91*, 27.

(16) Glauber, R. J. *Phys. Rev.* **1963**, *130*, 2529.

(17) Jezek, E.; Makri, N. *J. Phys. Chem.* **2001**, *105*, 2851.

(18) Makri, N. *J. Phys. Chem. B* **2002**, *106*, 8390.

(19) Yamamoto, T.; Wang, H.; Miller, W. H. *J. Chem. Phys.* **2002**, *116*, 7335.

(20) Feynman, R. P. *Statistical Mechanics*; Addison-Wesley: Redwood City, CA, 1972.

(21) Wright, N. J.; Makri, N. *J. Chem. Phys.* **2003**, *119*, 1634.

(22) Lawrence, C. P.; Nakayama, A.; Makri, N.; Skinner, J. L. *J. Chem. Phys.* **2004**, *120*, 6621.

(23) Ceperley, D. M. *Rev. Mod. Phys.* **1995**, *67*, 279.

(24) Nakayama, A.; Makri, N. *J. Chem. Phys.* **2003**, *119*, 8592.

CT1004356